Three-dimensional dynamics of a particle with a finite energy of magnetic anisotropy in a rotating magnetic field

J. Cīmurs and A. Cēbers*
University of Latvia, Zeļļu-8, Rīga, LV-1002, Latvia
(Received 2 October 2013; published 27 December 2013)

A model of a single ferromagnetic particle with a finite coupling energy of the magnetic moment with the body of the particle is formulated, and regimes of its motion in a rotating magnetic field are investigated. Regimes are possible that are synchronous and asynchronous with the field. In a synchronous regime the easy axis of the particle is in the plane of the rotating magnetic field at low frequencies (a planar regime) and on the cone at high frequencies (a precession regime). The stability of these regimes is investigated, and it is shown that the precession regime is stable for field strengths below the critical value. In a particular range of field strength value, irreversible jumps of the magnetic moment take place in the asynchronous planar regime. The stability of this regime is investigated, and it is shown that it is stable for field strengths above the critical value, which depends on the frequency. The implications of these results for the energy dissipation in a rotating field are analyzed, and it is shown that the maximum of the heat production near the transition to the synchronous regime is flattened out by the transition to the precession regime.

DOI: 10.1103/PhysRevE.88.062315 PACS number(s): 83.80.Gv, 47.65.Cb, 75.50.Mm, 75.60.Ej

I. INTRODUCTION

The dynamics of magnetic particles in AC magnetic fields plays an important role in different phenomena and applications. The technique of magnetic hyperthermia uses energy dissipated by the motion of magnetic particles in an AC field for cancer therapy [1–3]. The heat production due the hysteresis loop of the magnetic moment of the particle is considered in [4], and the role of thermal fluctuations of the magnetic moment in generating heat under the action of a rotating magnetic field is considered in [5]. Interesting structures are formed by superparamagnetic platelets in precessing magnetic fields [6]. It was predicted that magnetotactic bacteria in a rotating magnetic field should follow complex trajectories [7], which were also found in experiments [8]. In [8], when describing the experimentally observed behavior of magnetotactic bacteria, it was suggested, based on earlier work by Pincus and Caroli [9], that three-dimensional trajectories of a bacterium are possible in a rotating magnetic field due to the finite coupling energy of the magnetic moment of the bacterium to its cytoskeleton. In [9] it was shown that the ferromagnetic particle with an easy axis of magnetization in a well defined range of frequencies of a rotating field has a precession regime, in which its easy axis rotates on the cone with its angle depending on the ratio of the effective anisotropy field and the field strength. For some ranges of parameters the coexistence of the precession and planar solutions was predicted in [9]. Nevertheless, the phase diagram of the regimes of motion of a particle with a finite coupling energy of the magnetic moment to the particle remains unexplored. This problem is quite complicated due to the so-called rotational hysteresis phenomenon [10], taking place in a definite range of external field strength and not considered in [9].

Here the transition between the planar and precession regimes is considered by linear stability analysis, taking into account irreversible jumps of the magnetic moment due to rotational hysteresis, and the phase diagram for the regimes of particle motion is constructed, which was not known before. Its implication for the phenomenon of magnetic hyperthermia and experiments with suspensions of ferromagnetic particles in rotating magnetic fields are considered.

II. MODEL

The energy of a single domain ferromagnetic particle with an easy axis of magnetization is given by

$$E = -mH\vec{e}\cdot\vec{h} - \tfrac{1}{2}KV(\vec{e}\cdot\vec{n})^2, \tag{1}$$

where $\vec{e},\vec{n}$ are unit vectors along the magnetic moment and the easy axis respectively, $\vec{h}$ is the unit vector along the field, K is the constant of magnetic anisotropy, and V is the volume of the particle. Since the internal magnetic relaxation time is much smaller than the characteristic time of the particle motion, the magnetic moment is in an equilibrium state determined by $(\vec{K}_e = \vec{e}\times\partial/\partial\vec{e})\ \vec{K}_e E = 0$. It gives

$$\vec{e}\times\vec{h} = \frac{H_a}{H}(\vec{e}\cdot\vec{n})\vec{n}\times\vec{e}, \tag{2}$$

where $H_a = KV/m$. The dynamics of the easy axis is determined by the balance of viscous and mechanical torques and reads $(\vec{K}_n = \vec{n}\times\partial/\partial\vec{n})$

$$-\zeta\vec{\Omega} - \vec{K}_n E = 0, \quad \frac{d\vec{n}}{dt} = \vec{\Omega}\times\vec{n}, \tag{3}$$

where ζ is the rotational drag coefficient of the particle. Equation (3) for the angular velocity of the particle $\vec{\Omega}$ is the particular case of the more general "egg-yolk" model proposed in [11,12] and applied to the analysis of the nuclear magnetic relaxation dispersion in the presence of magnetic nanoparticles in [13], where it reads

$$\zeta\vec{\Omega} = -\vec{K}_e E - \vec{K}_n E. \tag{4}$$

Equation (3) describes the case when internal magnetic relaxation is neglected in Eq. (4).

*aceb@tesla.sal.lv

From (2) it follows that $\vec{e}$ is in the plane defined by the vectors $\vec{h}$ and $\vec{n}$:

$$\vec{e} = \frac{\vec{h} + \frac{H_a}{H}(\vec{e}\cdot\vec{n})\vec{n}}{\vec{e}\cdot\vec{h} + \frac{H_a}{H}(\vec{e}\cdot\vec{n})^2}, \tag{5}$$

where $(\vec{e}\cdot\vec{h})^2 = 1-(H_a/H)^2[1-(\vec{e}\cdot\vec{n})^2](\vec{e}\cdot\vec{n})^2$. For the given orientation angle φ of the external field with respect to the anisotropy axis, one or two stable states for the magnetic moment are possible depending on the value of H_a/H. Bifurcation occurs at $dE/d\vartheta = 0$ and $d^2E/d\vartheta^2 = 0$, where ϑ is the angle of the magnetic moment with the easy axis, which gives [14]

$$\cos^{2/3}\varphi + \sin^{2/3}\varphi = \left(\frac{H_a}{H}\right)^{2/3}. \tag{6}$$

From Eq. (6) it follows that transitions between situations with one or two stable states of the magnetic moment in a rotating magnetic field are possible if $1 < H_a/H < 2$. In this range of the magnetic field strength irreversible jumps of the magnetic moment can take place and should be taken into the account when the motion of the particle is considered. The orientation of the magnetic moment of the particle is found from the polynomial equation ($u = \vec{e}\cdot\vec{n}$)

$$(\vec{n}\cdot\vec{h})^2 + 2\vec{n}\cdot\vec{h}\frac{H_a}{H}u(1-u^2) + \left[\left(\frac{H_a}{H}\right)^2 - 1\right]u^2 - \left(\frac{H_a}{H}\right)^2 u^4 = 0, \tag{7}$$

which has two or four real solutions.

Introducing dimensionless time $\tilde{t}$ according to $\tilde{t} = \omega_H t$, where ω_H is a frequency of rotating field, the equation of the particle motion reads ($\omega_c = mH/\zeta$), tilde is omitted henceforth

$$\frac{d\vec{n}}{dt} = \frac{\omega_c}{\omega_H}C(\vec{n}\cdot\vec{h}, H_a/H, \xi)[\vec{h} - \vec{n}(\vec{n}\cdot\vec{h})], \tag{8}$$

where the function

$$C(\vec{n}\cdot\vec{h}, H_a/H, \xi) = \frac{H_a/H(\vec{e}\cdot\vec{n})_\xi^2}{\vec{n}\cdot\vec{h} + H_a/H(\vec{e}\cdot\vec{n})_\xi} \tag{9}$$

in general depends on the history due to the rotational hysteresis. The variable ξ, which has the values 1 or 2 depending on sign of $\vec{e}\cdot\vec{n}$, takes into the account the rotational hysteresis. The history-dependent $\vec{e}\cdot\vec{n}$ for the particular value of $H_a/H = 1.9$ as a function of $\vec{n}\cdot\vec{h}$ as given by Eqs. (6) and (7) is shown in Fig. 1. Irreversible jumps of the magnetic moment occur for this particular value of field strength at $(\vec{n}\cdot\vec{h})_1 = -0.48992$ and $(\vec{n}\cdot\vec{h})_2 = 0.48992$.

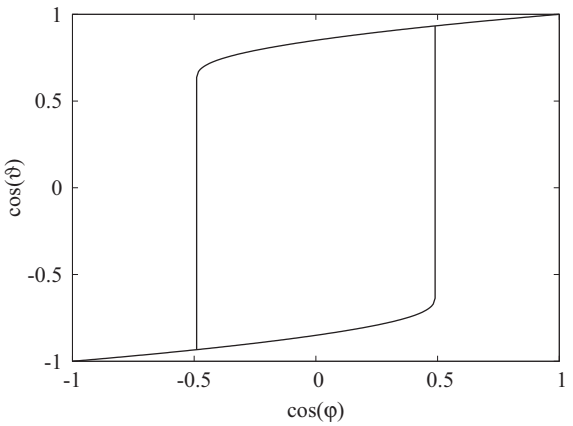

FIG. 1. History-dependent $\cos\vartheta = \vec{e}\cdot\vec{n}$ for the particular value of $H_a/H = 1.9$ as a function of $\cos\varphi = \vec{n}\cdot\vec{h}$.

III. STATIONARY REGIMES

Looking for the stationary regime in a rotating field $\vec{h} = (\cos t, \sin t, 0)$, when the particle rotates with the angular velocity of the field $\vec{\omega} = (0,0,1)$, $d\vec{n}/dt = \vec{\omega}\times\vec{n}$ from Eq.(8), we have

$$\frac{(\vec{e}\cdot\vec{n})^2(\vec{e}_z\cdot\vec{n})(\vec{n}\cdot\vec{h})}{\vec{n}\cdot\vec{h} + H_a/H(\vec{e}\cdot\vec{n})} = 0. \tag{10}$$

This equation is satisfied for $\vec{e}_z\cdot\vec{n} = 0$, which corresponds to the planar regime, or $\vec{n}\cdot\vec{h} = 0$, which corresponds to the precession regime. In the last case from Eq. (7) it follows that $(\vec{e}\cdot\vec{n})^2 = 1-(H/H_a)^2$, which implies that the precession regime is possible at $H < H_a$. The condition of the precessional motion

$$\vec{\omega}\times\vec{n} = \frac{\omega_c}{\omega_H}(\vec{e}\cdot\vec{n})\vec{h} \tag{11}$$

then gives

$$1-\cos^2\gamma = \left(\frac{\omega_c}{\omega_H}\right)^2\left[1-\left(\frac{H}{H_a}\right)^2\right], \tag{12}$$

where γ is the angle of a cone with axis along the z axis, on which moves the vector $\vec{n}$ in the precession regime. That gives the second condition for the existence of the precession regime,

$$0 < \left(\frac{\omega_c}{\omega_H}\right)^2\left[1-\left(\frac{H}{H_a}\right)^2\right] < 1. \tag{13}$$

These two conditions were found in [9]. A sketch of the particle easy axis and magnetic field orientations in the precession regime is shown in Fig. 2. The boundary of the region defined by (13) introducing field-independent critical frequency $\omega_a = mH_a/2\zeta$ is shown in Fig. 3 by a solid line.

In principle, a stationary state exists in the case $H_a/H < 1$, where the easy axis is along $\vec{\omega}$ and magnetic moment is along

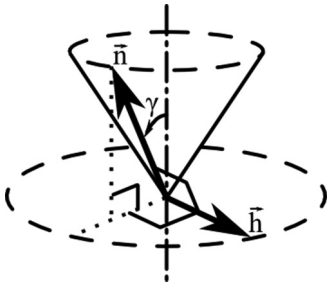

FIG. 2. Orientations of easy axis and magnetic field in the precession regime.

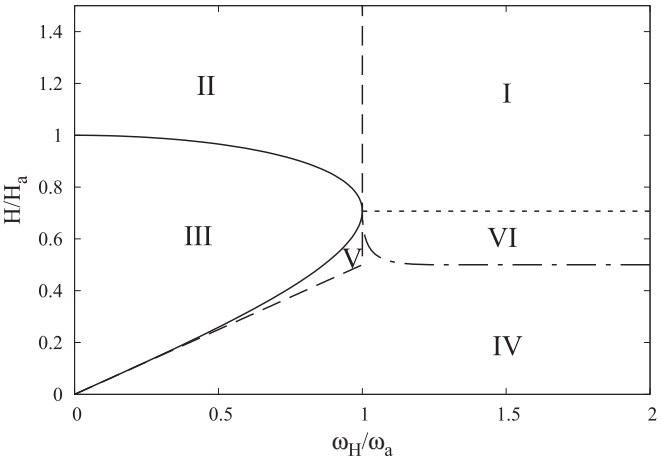

FIG. 3. Phase diagram. The solid line indicates the boundary of the region where the precession regime exists; the dashed line is the boundary of the existence region of the stationary planar regime; the dotted line is the neutral curve of stability of the precession regime; the dash-dotted line is the neutral curve of stability of the nonstationary planar regime. The precession regime is stable in the region IV $\bigcup$ V $\bigcup$ VI and unstable in the region I $\bigcup$ II. The stationary planar regime is stable in the region II $\bigcup$ III and unstable in the region V. The nonstationary planar regime is stable in the region I $\bigcup$ VI and unstable in the region IV.

the instantaneous direction of the field. Equation (8) and (9) and relation $(\vec{e}\cdot\vec{n})(\vec{e}\cdot\vec{h}) = \vec{n}\cdot\vec{h} + H_a/H(\vec{e}\cdot\vec{n})[1-(\vec{e}\cdot\vec{n})^2]$ give the equation for a small perturbation of this state $\vec{n}'$,

$$\frac{d\vec{n}'}{dt} = \frac{\omega_c}{\omega_H}\frac{H_a}{H-H_a}(\vec{n}'\cdot\vec{h})\vec{h}. \tag{14}$$

Equation (14) shows that the state with the easy axis parallel to the angular velocity vector of the field at $H_a/H < 1$ is unstable.

In the limit $H \to 0$ the model approaches the model of a rigid dipole. In this case, for $\omega_H > \omega_c$ three-dimensional periodic trajectories are possible, which correspond to the center in the plane of dynamical variables of the system [15,16]. This case is structurally unstable and a small perturbation of the system destroys it. The role of the perturbation in the present case is played by small deviations of the magnetic moment from the easy axis, and as a result the precession regime is established in the region $H_a/H > 2$ and $\omega_H/\omega_c > 1$. The memory of the existence of three-dimensional trajectories is reflected by the stage of the transition to the stationary precession regime. It should be remarked that a similar phenomenon takes place if we introduce a field component along the angular velocity of field rotation as a small perturbation, which corresponds to the precessing magnetic field [17].

Next we explore stability of the precession regime, which to our knowledge has never been done. It is convenient to introduce angles α and δ, which characterize the orientation of the easy axis $\vec{n} = (\cos\alpha\cos\delta, \cos\alpha\sin\delta, \sin\alpha)$. Equation (8) gives

$$\dot{\beta} = 1 - \frac{\omega_c}{\omega_H}\frac{C(\vec{n}\cdot\vec{h})\sin\beta}{\cos\alpha}, \tag{15}$$

$$\cos\alpha\dot{\alpha} = -\frac{\omega_c}{\omega_H}C(\vec{n}\cdot\vec{h})\sin\alpha\vec{n}\cdot\vec{h}, \tag{16}$$

where $\beta = t - \delta$ is the phase lag with the external field. In the precession regime $\vec{n}\cdot\vec{h} = 0$, which gives $\beta_0 = \pi/2$, and $C = C_0 = \pm\sqrt{1-(H/H_a)^2}$, $\cos\alpha_0 = C_0\omega_c/\omega_H$. For small perturbations (β',α') of the state (β_0,α_0) we have $(\vec{n}\cdot\vec{h})' = -\cos\alpha_0\beta'$, which gives

$$\dot{\alpha}' = \frac{\omega_c}{\omega_H}C_0\sin\alpha_0\beta'. \tag{17}$$

The derivation of the equation for β' is a bit more complicated. From Eq. (14) we have

$$\dot{\beta}' = -\frac{\omega_c}{\omega_H}\frac{C'}{\cos\alpha_0} - \frac{\omega_c}{\omega_H}\frac{C_0\alpha'}{\cos^2\alpha_0}. \tag{18}$$

Using relation (9) we obtain

$$C' = (\vec{e}\cdot\vec{n})' - \frac{H}{H_a}(\vec{n}\cdot\vec{h})'. \tag{19}$$

Differentiation of Eq. (7) gives

$$(\vec{e}\cdot\vec{n})' = -\frac{(\vec{n}\cdot\vec{h})'}{H_a/H(1-(H_a/H)^2)} \tag{20}$$

and

$$C' = \frac{2-(H_a/H)^2}{H_a/H(1-(H_a/H)^2)}\cos\alpha_0\beta'. \tag{21}$$

As a result we obtain a set of linear differential equations

$$\dot{\beta}' = -a\beta' - \frac{1}{\cos\alpha_0}\alpha', \tag{22}$$

$$\dot{\alpha}' = \cos\alpha_0\sin\alpha_0\beta', \tag{23}$$

where

$$a = \frac{\omega_c}{\omega_H}\frac{2-(H_a/H)^2}{H_a/H(1-(H_a/H)^2)}.$$

For the growth increments of small perturbations λ this result gives

$$2\lambda = -a \pm \sqrt{a^2 - 4\sin^2\alpha_0}.$$

Since $4\sin^2\alpha_0 > 0$ instability takes place at $a < 0$, which corresponds to the range of magnetic field $1 < H_a/H < \sqrt{2}$, since $H_a/H > 1$ from the condition of the existence of the precession regime. The neutral curve of the precession regime $H/H_a = 1/\sqrt{2}$ is shown in Fig. 3 by a dotted line. It limits the region of parameters in which the precession regime is stable.

As a next step we consider the condition for the existence of the stationary planar solution. From Eqs. (2) and (3) follows that in the case of a stationary planar solution

$$\vec{e}_z = \frac{\omega_c}{\omega_H}\frac{H_a}{H}(\vec{e}\cdot\vec{n})\vec{n}\times\vec{e}. \tag{24}$$

Since $\vec{e}\cdot\vec{n} = \cos\vartheta$ and $\vec{n}\times\vec{e} = \sin\vartheta\vec{e}_z$, a stationary planar solution exists if

$$\frac{\omega_c}{\omega_H}\frac{H_a}{H} > 2. \tag{25}$$

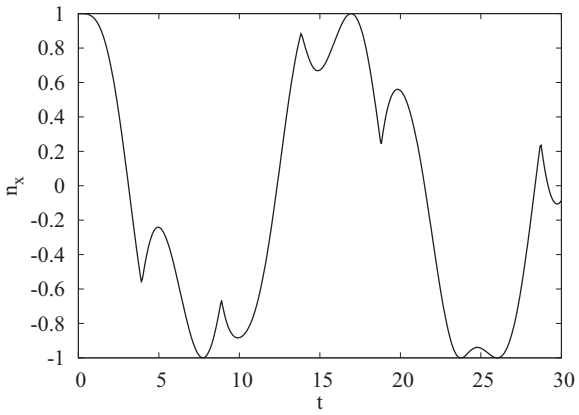

FIG. 4. n_x as a function of time in the nonstationary planar regime at $\frac{H}{H_a} = 0.67$ and $\frac{\omega_H}{\omega_a} = 1.33$.

On the other hand Eqs. (2) and(24) give $\vec{e}_z = \omega_c/\omega_H \vec{e} \times \vec{h}$. Since for the planar solution $\vec{e} \times \vec{h} = \sin\varphi \vec{e}_z$ we obtain the second condition $\omega_c/\omega_H > 1$. The boundary of the region of the existence of stationary planar solutions given by $\omega_H/\omega_a = 1$ and $\omega_H/\omega_a = H/2H_a$ is shown in Fig. 3 by the dashed line. It is tangent to the boundary of the region of existence of the precession regime given by (13) at the point $\omega_H/\omega_a = 1$, $H/H_a = 1/\sqrt{2}$. In the region between the solid and dashed lines in Fig. 3 both planar and precession regimes exist, and the precession regime is stable at $H/H_a < 1/\sqrt{2}$.

At $\omega_H/\omega_a > 1$ the nonstationary planar solution with irreversible jumps of the magnetic moment exists when $0.5 < H/H_a < 1$, as illustrated by Figs. 4 and 5, where numerically calculated $n_x(t)$ and $\vec{e} \cdot \vec{n}(t)$ are shown for $\frac{H}{H_a} = 0.67$ and $\frac{\omega_H}{\omega_a} = 1.33$. Since in this region of the parameter space also the precession regime exists, we further investigate the stability of the nonstationary planar solution. Considering small perturbations of the angle α of the planar regime with $\alpha_0 = 0$, Eq.(15) gives

$$\dot{\alpha}' = -\frac{\omega_c}{\omega_H} C(\vec{n}_0 \cdot \vec{h}, \xi) \vec{n}_0 \cdot \vec{h} \alpha', \tag{26}$$

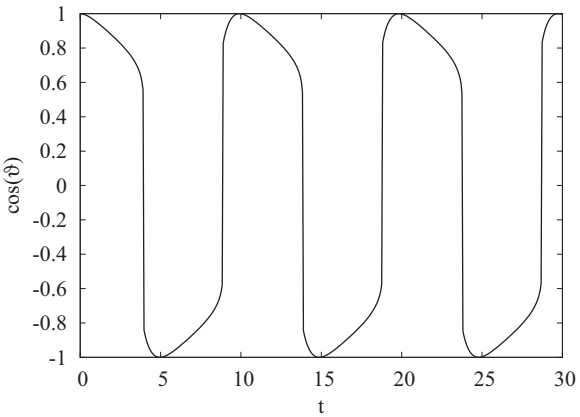

FIG. 5. $\cos\vartheta = \vec{e} \cdot \vec{n}$ as a function of time in the nonstationary planar regime at $\frac{H}{H_a} = 0.67$ and $\frac{\omega_H}{\omega_a} = 1.33$.

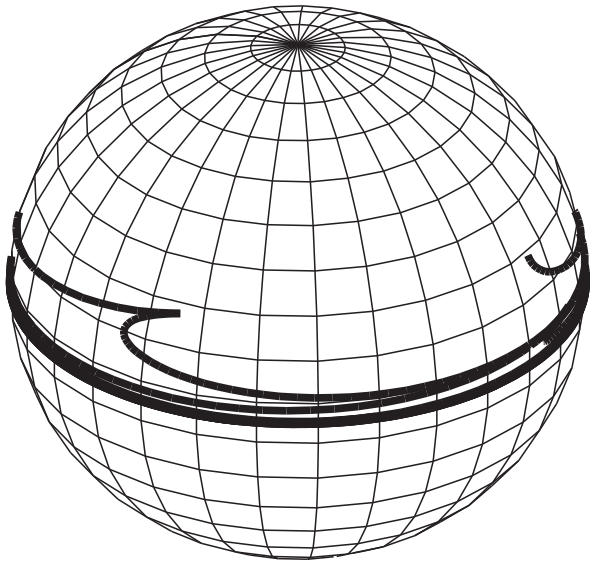

FIG. 6. Trajectory of $\vec{n}$ at $\frac{\omega_H}{\omega_a} = 1.16$ and $\frac{H}{H_a} = 0.529$ with starting conditions $\vec{n} \cdot \vec{h} = 0.92$ and $\vec{n} \times \vec{h} \perp \vec{e}_z$. The solution approaches the nonstationary planar regime.

where $\vec{n}_0 \cdot \vec{h} = \cos\beta_0$ and β_0 satisfies the equation

$$\dot{\beta}_0 = 1 - \frac{\omega_c}{\omega_H} C(\cos\beta_0, \xi) \sin\beta_0. \tag{27}$$

As a result the Floquet multiplier λ_F of the Eq. (26) with the periodic-in-time coefficient reads

$$\lambda_F = \exp\left(-\int_0^T \frac{\omega_c}{\omega_H} C(\cos\beta_0, \xi) \sin\beta_0 dt \right), \tag{28}$$

where $\alpha'(T) = \lambda_F \alpha'(0)$, and T is the period. Taking into account the irreversible jumps of the magnetic moment and Eq. (27), we see that the stability of the nonstationary planar solution is determined by the sign of the integral

$$I_0\left(\frac{\omega_c}{\omega_H}, \frac{H_a}{H}\right) = \int_0^{\pi/2+\varphi_1} f_1\left(\frac{\omega_c}{\omega_H}, \frac{H_a}{H}, t\right) d\beta + \int_{\pi/2+\varphi_1}^{\pi} f_2\left(\frac{\omega_c}{\omega_H}, \frac{H_a}{H}, t\right) d\beta, \tag{29}$$

where

$$f_{1,2} = \frac{\omega_c}{\omega_H} \frac{C(\cos\beta, (1,2)) \cos\beta}{1 - \frac{\omega_c}{\omega_H} C(\cos\beta, (1,2)) \sin\beta},$$

and $\varphi_1 < \pi/4$ is the root of Eq. (6). Curve $I_0(\frac{\omega_c}{\omega_H}, \frac{H_a}{H}) = 0$ is shown in coordinates $\omega_H/\omega_a, H/H_a$ by the dash-dotted line in Fig. 3. Below this line the nonstationary planar solution is unstable and the precession regime is established. The direct numerical solution of Eq. (8) confirms this as illustrated in Figs. 6 and 7 by the three-dimensional phase portraits of the unit vector $\vec{n}$ on the sphere for values of H_a/H slightly above and below the critical value given by $I_0(\frac{\omega_c}{\omega_H}, \frac{H_a}{H}) = 0$. Numerical calculations were carried out using MATLAB solver ode15s with relative tolerance equal to 10^{-10}. The history-dependent magnetic state of the particle was taken into account by the value of variable ξ as

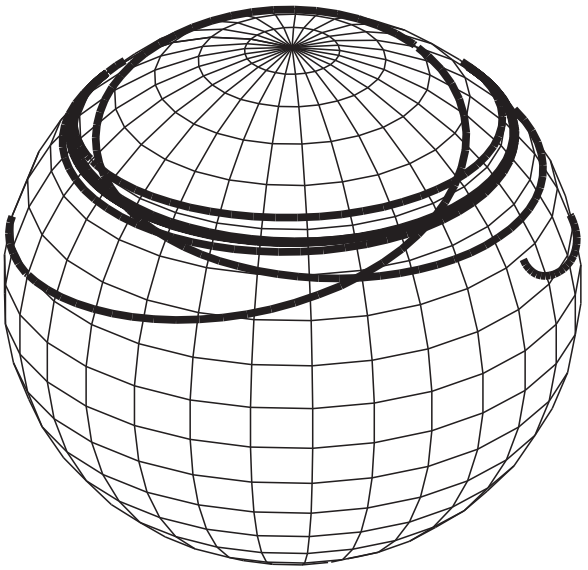

FIG. 7. Trajectory of $\vec{n}$ at $\frac{\omega_H}{\omega_a} = 1.16$ and $\frac{H}{H_a} = 0.526$ with starting conditions $\vec{n}\cdot\vec{h} = 0.92$ and $\vec{n}\times\vec{h} \perp \vec{e}_z$. The solution approaches the precession regime.

described above. Stable precession and planar regimes coexist in the region between the dash-dotted and dotted lines in Fig. 3.

IV. ENERGY DISSIPATION AND TORQUE CURVES

The model allows us to consider in detail the heat production and torque on the suspension of ferromagnetic particles in a rotating field due to the viscous friction and irreversible jumps of the magnetic moment of the particle. Equations (1) and (3) give

$$\frac{dE}{dt} = -mH\frac{d\vec{e}}{dt}\left(\vec{h} + \frac{H_a}{H}\vec{n}\vec{e}\cdot\vec{n}\right) - mH\vec{e}\cdot\frac{d\vec{h}}{dt} - \zeta\vec{\Omega}^2. \quad (30)$$

The first term in Eq. (30) is zero for quasistatic changes of the magnetic moment of the particle, and gives a finite contribution for its irreversible jumps. As a result for the mean energy dissipated per period T we have

$$\left\langle -mH\vec{e}\cdot\frac{d\vec{h}}{dt}\right\rangle = \zeta\langle\vec{\Omega}^2\rangle + \frac{(E_1 - E_2)n}{T}, \quad (31)$$

where $n = 2$ is the number of irreversible jumps per period and $E_1, E_2 (E_1 > E_2)$ are the energies of the particle before and after the jump, respectively. The relation (31) in the case of the precession regime when jumps of the magnetic moment do not take place gives

$$\zeta\langle\vec{\Omega}^2\rangle = \zeta\omega_c^2(1 - 1/(H_a/H)^2). \quad (32)$$

Introducing as the characteristic scale of energy dissipation $\zeta\omega_c^2$, relation (32) for the dimensionless heat production in the precession regime gives $1 - 1/(H_a/H)^2$. It does not depend on the frequency and is valid in the frequency region where the stable precession regime exists.

In the region below the neutral curve of the nonstationary planar regime shown in Fig. 3 by the dash-dotted line and

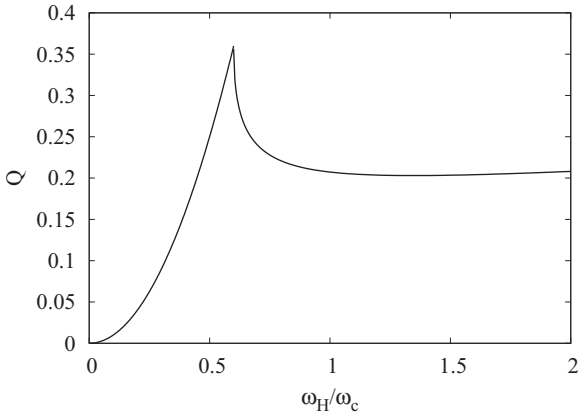

FIG. 8. Average energy supplied by field as function of rotation frequency at $\frac{H}{H_a} = 0.83$.

$H/H_a < 1/\sqrt{2}$, both nonstationary and precession regimes coexist. Energy dissipated in the nonstationary regime is calculated numerically according to the relation

$$\left\langle -mH\vec{e}\cdot\frac{d\vec{h}}{dt}\right\rangle = \zeta\omega_H^2\vec{e}_z\cdot\langle\vec{n}\times\dot{\vec{n}}\rangle. \quad (33)$$

It is checked numerically that the energy balance is fulfilled, which, written in dimensionless form, reads ($\tilde{E} = E/mH$)

$$Q = \frac{\omega_H^2}{\omega_c^2}\vec{e}_z\cdot\langle\vec{n}\times\dot{\vec{n}}\rangle = \frac{\langle\vec{\Omega}^2\rangle}{\omega_c^2} + n\frac{\omega_H}{\omega_c}\frac{(\tilde{E}_1 - \tilde{E}_2)}{\tilde{T}}. \quad (34)$$

Thus, in the nonstationary planar regime the energy supplied by the field is dissipated by the viscous friction and hysteresis losses of the particle when irreversible jumps of the magnetic moment take place. The numerically calculated dissipated energies for two values of H/H_a are shown in Fig. 8 ($H/H_a = 0.83$) and Fig. 9 ($H/H_a = 0.53$). In the first case, when $H/H_a > 1/\sqrt{2}$, the precession regime is not stable and the heat is produced in the nonstationary planar regime. The maximum is observed at the frequency at which the transition to the stationary regime takes place. At high frequencies the

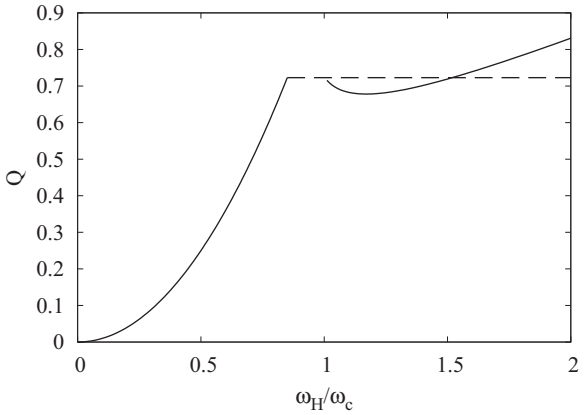

FIG. 9. Average energy supplied by field as function of rotation frequency at $\frac{H}{H_a} = 0.526$. Solid lines correspond to planar regimes. The dashed line corresponds to the precession regime.

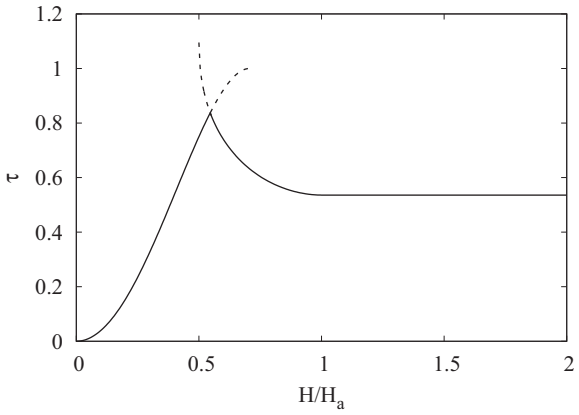

FIG. 10. Torque in dependence on the field strength. $\omega_H/\omega_a = 2$. The left curve shows the torque for the precession regime, the right curve shows the torque for the planar asynchronous regime. Torques in the precession and planar regimes where both regimes coexist are shown by dashed lines.

energy dissipated in the particle prevails. In the second case ($H/H_a = 0.53$) the planar and precession regimes coexist at $\omega_H > \omega_H^*$, where ω_H^* is given by the neutral curve of the nonstationary planar regime in Fig. 3. In Fig. 9 the heat produced in the precession regime is shown by the dashed line and in the planar regime by the solid line. Since only the precession regime is stable above the neutral curve of the planar regime, the maximum shown in Fig. 8 is flattened out. At low frequencies the energy is dissipated in the stationary planar regime.

In experiments the rotational hysteresis usually is studied by measurements of the torque on a suspension as a function of the rotating field strength [18] (for a review see [16]). The dimensionless torque $\tau = N/\zeta\omega_H$ is related to the energy dissipation according to the relation $\tau = \omega_c^2 Q/\omega_H^2$. Torques acting on a suspension in precession and asynchronous planar regimes at $\omega_H/\omega_a = 2$ are shown in Fig. 10. Since at this particular frequency there is a range of field strength values where both regimes coexist, the torque curves in the region of coexistence are continued by dashed lines. An important feature of the torque curve is the existence of a maximum at a field strength $H/H_a \simeq 0.5$. This is in the agreement with experimental data for the suspension of elongated particles of γ-Fe_2O_3 reported in [19]. Taking into account that the magnetic anisotropy of elongated particles is due to their shape, the constant of magnetic anisotropy may be estimated by $K = 2\pi M^2$, which for the anisotropy field gives $H_a = 2\pi M$. Taking the saturation magnetization of γ-Fe_2O_3 as 500 G for $H_a/2$ we have 1.5 kOe, which is close to the field strength at which the maximum of the torque curve is observed. Since the maximum of the torque of liquid suspension is found at approximately the same value of the magnetic field strength as for the solidified suspension [19] then we have evidence that the maximum is due to the rotational hysteresis. It is interesting to remark that the part of the torque curve at small field strength values given in [19] can be very well matched by the expression for the torque corresponding to the precession regime $\tau = 4\omega_a^2(H/H_a)^2[1-(H/H_a)^2]/\omega_H^2$, which has a maximum at $H/H_a \simeq 0.7$.

V. CONCLUSIONS

It is shown that synchronous and asynchronous regimes are possible for a particle with a finite energy of the magnetic anisotropy in a rotating magnetic field. In the synchronous regime the easy axis of the particle is in the plane of a rotating field at low frequencies (a planar regime) and on the cone (a precession regime) at high frequencies. The stability of both regimes is investigated and it is shown that the precession regime is stable for the magnetic field strength below the critical value. Taking into account irreversible jumps of the magnetic moment it is shown that the planar asynchronous regime is unstable for the field strength below the critical value, which depends on the frequency. Analysis of the heat production by the particle in a rotating field shows that the maximum of the energy dissipation near the transition to the synchronous regime is flattened out due to the transition to the precession regime.

ACKNOWLEDGMENTS

This work was supported by 7th European Framework Project Bio2Man4MRI (Grant No. 245542).

[1] J. P. Fortin, C. Wilhelm, J. Servais, Ch. Menager, J.-C. Bacri, F. Gazeau, J. Am. Chem. Soc. **129**, 2628 (2007).
[2] C. Wilhelm and F. Gazeau, J. Magn. Magn. Mater. **321**, 671 (2009).
[3] R. E. Rosensweig, J. Magn. Magn. Mater. **252**, 370 (2002).
[4] R. Hergt, R. Hiergeist, M. Zeisberger, D. Shuler, U. Heyden, I. Hilger, and W. A. Kaiser, J. Magn. Magn. Mater. **293**, 80 (2005).
[5] Yu. L. Raikher, and V. I. Stepanov, Phys. Rev. E **83**, 021401 (2011).
[6] J. Yan, M. Bloom, S. C. Bac, E. Luijten, and S. Granick, Nature (London) **491**, 578 (2012).
[7] H. Tanaka, M. Isobe, and H. Miyazawa, Phys. Rev. E **73**, 021503 (2006).
[8] K. Erglis, Qi Wen, V. Ose, A. Zeltins, A. Sharipo, P. A. Janmey, and A. Cebers, Biophys. J. **93**, 1402 (2007).
[9] C. Caroli, and P. Pincus, Phys. Kondens. Mater. **9**, 311 (1969).
[10] B. Kashevsky, Magnetohydrodynamics **11** (4), 37 (1975).
[11] M. I. Shliomis and V. I. Stepanov, J. Magn. Magn. Mater. **122**, 196 (1993).
[12] M. I. Shliomis and V. I. Stepanov, J. Magn. Magn. Mater. **122**, 176 (1993).
[13] R. Taukulis and A. Cebers, Phys. Rev. E **86**, 061405 (2012).

[14] L. D. Landau and E. M. Lifshitz, *Electrodynamics of Continuos Media* (Pergamon, Oxford, 1960).
[15] E. J. Hinch and L. G. Leal, J. Fluid Mech. **52**, 683 (1972).
[16] E. Blums, A. Cebers, and M. M. Maiorov, *Magnetic Liquids* (W. de Gruyter, Berlin, 1997).
[17] J. Cīmurs and A. Cēbers, Phys. Rev. E **87**, 062318 (2013).
[18] I. S. Jacobs and F. E. Luborsky, J. Appl. Phys. **28**, 467 (1957).
[19] S. R. Gorodkin, B. E. Kashevskii, V. I. Kordonskii, and I. V. Prokhorov, Tech. Phys. Lett. **10**, 94 (1984).